

M. Asteazaran <sup>a</sup>, G. Cespedes <sup>b</sup>, M.S. Moreno <sup>c</sup>, S. Bengió <sup>c</sup>,  
A.M. Castro Luna <sup>a,b,\*</sup>

<sup>a</sup> Instituto de Investigaciones Fisicoquímicas Teóricas y Aplicadas (INIFTA), Facultad de Ciencias Exactas, UNLP-CONICET, La Plata, Argentina

<sup>b</sup> Centro de Investigación y Desarrollo en Ciencia y Tecnología de Materiales (CITEMA), Facultad Regional La Plata, UTN, La Plata, Argentina

<sup>c</sup> Centro Atómico Bariloche, Comisión Nacional de Energía Atómica (CAB-CNEA) and CONICET, San Carlos de Bariloche, Argentina

---

#### A B S T R A C T

Trimetallic PtMRu/C cathode catalysts with M = Co or Fe obtained by an impregnation procedure using ethylene glycol and NaBH<sub>4</sub> as reducing agent, with suitable activity for the oxygen reduction reaction (ORR) and improved tolerance to methanol, have been physically characterized by HRTEM, EDS and XPS. The examined nanoparticles have a small particle size and are well spread on the carbon support. Pt is mainly found as Pt(0) and Co, Fe and Ru are mostly oxidized. To study their durability and performance for ORR and methanol tolerance over time, the catalysts were subjected to an electrochemical accelerated stress test (AST), consisting in cycling the potential 2000 times. Polarization curves for ORR with and without methanol were recorded. After the AST the trimetallic PtMRu/C catalysts are able to keep their performance for ORR in the presence of methanol.

Keywords:

ORR

Methanol crossover

Methanol-tolerant catalyst

Passive direct methanol fuel cells

Accelerated stress test

Trimetallic catalysts

---

## Introduction

Proton exchange membrane fuel cells (PEMFCs) are promising electrochemical devices that convert the fuel-chemical energy into electrical energy in a clean and efficient way. Among PEMFCs, direct methanol fuel cells (DMFCs) have become increasingly attractive because they utilize a liquid fuel at the anode that has high density energy and is easy to handle,

store and transport. In portable applications, passive DMFCs are one of the most prospective power sources [1–3].

In passive DMFCs, methanol, water and oxygen are passively supplied from the methanol container and from the air to the membrane electrode assembly (MEA) by capillary forces, gravity and concentration gradients thus, making it unnecessary to use auxiliary components, which consume part of the energy generated, for feeding reagents to the cell. Passive DMFCs require the use of high alcohol concentration to feed the anode. Consequently, a technical obstacle to

---

\* Corresponding author.

E-mail addresses: [castrolu@inifta.unlp.edu.ar](mailto:castrolu@inifta.unlp.edu.ar), [castrolu@gmail.com](mailto:castrolu@gmail.com) (A.M. Castro Luna).

overcome in these devices is methanol crossover, a phenomenon in which methanol diffuses from the anode to the cathode through the Nafion<sup>®</sup> membrane dragged by water because of the miscibility between methanol and water [1,4]. The crossover of methanol causes a considerable loss of fuel cell efficiency, since both the oxygen reduction reaction (ORR) and the methanol oxidation reaction (MOR) occur simultaneously on the cathode. Pt is the most widely employed cathode catalyst for the ORR, though its catalytic activity towards the oxygen reduction reaction is still insufficient [5].

One approach to solving the alcohol crossover issue in DMFCs consists in the substitution of Pt by a catalyst with high activity for the ORR and low activity for the MOR [6]. Many attempts to improve the cathode performance for the ORR, such as the employment of Pt-based catalysts with transition metals that change Pt oxophilicity and electron availability, have been successfully made [5,7–10]. Despite the amount of research carried out to establish the role of co-catalysts in the kinetic improvement of ORR, no definitive conclusion has been reached yet [11]. One of the difficulties to determine the effect of transition metals on ORR improvement is that the activity of a supported catalyst has a wide range of values depending on its microstructure and preparation procedure [4,12–15]. It has been claimed that a selective dissolution of the less-noble component from the nanoparticles (NPs) typically results in either the formation of coreshell structures or porous noble-metal-rich NPs with higher catalytic activity for ORR [16]. Summarizing, the intrinsic activity of NPs depends on their particle size, shape, composition, etc. [15,17].

In our previous works related to the search of a methanol-tolerant cathode catalyst for DMFCs, we built bimetallic PtCo/C and PtFe/C catalysts with a noteworthy performance for ORR, and trimetallic PtCoRu/C and PtFeRu/C catalysts that were also methanol-tolerant [18,19]. To obtain suitable cathode catalysts for passive DMFCs, it is important that the catalysts keep their electrochemical performance for ORR and their methanol-tolerance ability not only initially but over time. Therefore, once a suitable cathode catalyst with high methanol tolerance is obtained, long-time durability tests are required [20–22].

The aim of this work is to study the durability and performance of PtCoRu/C and PtFeRu/C synthesized methanol-tolerant cathode catalysts employing electrochemical accelerated stress tests (AST) to examine their catalytic behavior and methanol-tolerance decrease over time, prior to their widespread use in passive DMFCs.

## Experimental

### Catalyst preparation

Methanol-tolerant cathodes with suitable activity for ORR, i.e., PtMRu/C catalysts, with M = Co or Fe, were prepared by an impregnation method (IM) via seed-mediated growth, employing ethylene glycol and NaBH<sub>4</sub> as reducing agent; a more detailed description of the methodology is found in Refs. [23,19]. Briefly, in the IM procedure, H<sub>2</sub>PtCl<sub>6</sub>, MCl<sub>x</sub> (M = Fe and Co), RuCl<sub>3</sub> and functionalized carbon support (Vulcan<sup>®</sup> XC-72R) were dissolved separately in ethylene glycol and ultrasonicated under N<sub>2</sub> flow during the whole synthesis

procedure. Then, the pH was changed to 10 by adding NH<sub>4</sub>OH and subsequently, a small volume of the Pt precursor and 0.1 M NaBH<sub>4</sub> solution were added to form Pt seeds. After a few minutes, the remaining precursor and NaBH<sub>4</sub> solutions were added with further stirring for 2 h. The solid obtained by vacuum filtering was thoroughly washed and dried at 70 °C. The catalysts are denoted as PtMRu/C IM.

In this paper, a homemade PtCo/C catalyst that showed an outstanding behavior for ORR [18] is taken as comparison catalyst. We previously obtained the catalyst by a slightly modified impregnation method with a thermal treatment in a reducing atmosphere [24].

### Characterization

The distribution and size particles of the supported catalysts were examined by a Tecnai F20 G2 high resolution transmission electron microscope (HRTEM), their bulk compositions by energy-dispersive X-ray spectroscopy (EDS), and the surface composition and chemical state of the active components by X-ray photoelectron spectroscopy (XPS).

### Catalysts activity and durability evaluations

The electrochemical characterization of the synthesized catalysts was performed using a standard three-electrode electrochemical cell. A rotating disk electrode (RDE) of glassy carbon (0.071 cm<sup>2</sup> geometric area) covered with a thin layer of catalyst powder, attached by a 0.1 μm Nafion<sup>®</sup> thin film, was used as working electrode. The catalyst loading on the RDE was adjusted to 28 μg<sub>Pt</sub> cm<sup>-2</sup> therefore, the quantity of catalyst on the electrode was around 5 μg. A Pt foil of 1 cm<sup>2</sup> geometric area was used as counterelectrode and a saturated calomel electrode (SCE) as reference electrode. In this work, all potentials are referred to that of the reversible hydrogen electrode (RHE). The active area of Pt in cm<sup>2</sup><sub>Pt</sub> was obtained from the CO stripping assuming 420 μCcm<sup>-2</sup> for one monolayer oxidation of adsorbed carbon monoxide.

The working solution was an O<sub>2</sub>-saturated 0.5 M H<sub>2</sub>SO<sub>4</sub> solution with or without CH<sub>3</sub>OH. Though different alcohol concentrations were employed, the polarization curves are shown with 0.1 M CH<sub>3</sub>OH. The electrochemical experiments were conducted at room temperature. Previous to ORR experiments, the potential of a fresh working electrode was cycled at a rate of 0.1 Vs<sup>-1</sup> in a N<sub>2</sub>-purged 0.5 M H<sub>2</sub>SO<sub>4</sub> solution between 0.05 V and 0.8 V, until a stable voltammetric profile was attained. The polarization curves for ORR were recorded starting from the open circuit potential value up to 0.05 V at a scan rate of 0.005 Vs<sup>-1</sup> and a disk rotation rate ω = 2000 rpm. The current densities of the polarization curves shown were calculated taking into account the geometric area of the electrode.

Degradation of the catalysts was evaluated by cycling the electrode potential 2000 times between 0.05 and 0.8 V at 0.05 Vs<sup>-1</sup> under N<sub>2</sub> bubbling [25]. In addition, polarization curves for ORR before and after AST were recorded with and without CH<sub>3</sub>OH.

The onset potential for the ORR, at which the current for oxygen reduction is first observed, was determined by the point of intersection of two lines, one drawn extending the

baseline (i.e. from 1 V to 0.9 V) and the other extending the increasing linear portion of ORR polarization curve. The specific activity for ORR at 0.8 V was calculated as the kinetic current normalized by the active area in  $\text{cm}^2_{\text{Pt}}$  [26]; the kinetic current was determined using the mass-transport correction for thin-film RDEs following equation (1).

$$I_k = \frac{I_{\text{lim}} \cdot I}{(I_{\text{lim}} - I)} \quad (1)$$

where  $I_k$  is the kinetic current [A],  $I_{\text{lim}}$  is the measured limiting current [A] and  $I$  is the measured current to be corrected [A].

Besides, the electrochemically active surface area (ECSA) expressed in  $\text{m}^2 \text{g}_{\text{Pt}}^{-1}$  and calculated according to equation (2) [27] allows us to know the number of the electrochemically active sites on which the electrocatalytic reactions occur.

$$\text{ECSA} = \frac{Q_{\text{CO}} \cdot 100}{(420 \cdot \Gamma_{\text{Pt}})} \quad (2)$$

where  $Q_{\text{CO}}$  [C] is the integrated charge of CO stripping peak area after subtracting the charge from the double-layer region,  $\Gamma_{\text{Pt}}$  [g] is the Pt loading on the electrode, and 420 [ $\mu\text{Ccm}^{-2}$ ] is the charge required to oxidize a monolayer of CO on the Pt surface.

All parameters for ORR above described were determined before and after the AST.

## Results and discussion

### HRTEM images

HRTEM images of all the synthesized catalysts showed NPs uniformly spread on the carbon support Vulcan<sup>®</sup> XC-72R. The images and their histograms of particle size distribution are shown in Fig. 1 a, b and c for PtCo/C, PtCoRu/C IM and PtFeRu/C IM. HRTEM images of the NPs exhibit a mean particle size of 5.44 nm, 4.16 nm and 3.64 nm for PtCo/C, PtCoRu/C IM and PtFeRu/C IM, respectively. It is possible to conclude that trimetallic IM catalysts form smaller particles than the binary PtCo/C.

### XPS analysis

The Pt 4f, Ru 3d, Co 2p and Fe 2p XP spectra of PtCo/C, PtCoRu/C IM and PtFeRu/C IM are shown in Fig. 2 a, b and c, respectively.

The elemental Pt 4f core-level spectrum is composed of two peaks that correspond to the spin-orbit split  $4f_{7/2}$  and  $4f_{5/2}$ . The Pt 4f spectrum for PtCo/C shows a single doublet, whereas for both IM catalysts the Pt 4f spectra could be deconvoluted into two pairs of doublets. All analyzed catalysts exhibit a peak ascribed to Pt(0), which is at BE = 71.2 eV for PtCo/C, and at BE = 71.9 eV for the IM catalysts; for the latter their second Pt  $4f_{7/2}$  peak is at BE = 73.7 eV for PtCoRu/C and at 73.9 eV for PtFeRu/C, which could be attributed to the formation of an intermediate oxide [18]. It is worth noting that the peaks ascribed to Pt(0) are shifted apart almost 1 eV to more bounded states with respect to the nominal value of bulk Pt. This shift is probably due to a contribution from the metal-support interaction or effects due to the small size of NPs [28].

Furthermore, for PtCo/C and PtCoRu/C IM, the Co 2p spectra could barely be deconvoluted into two peaks in the

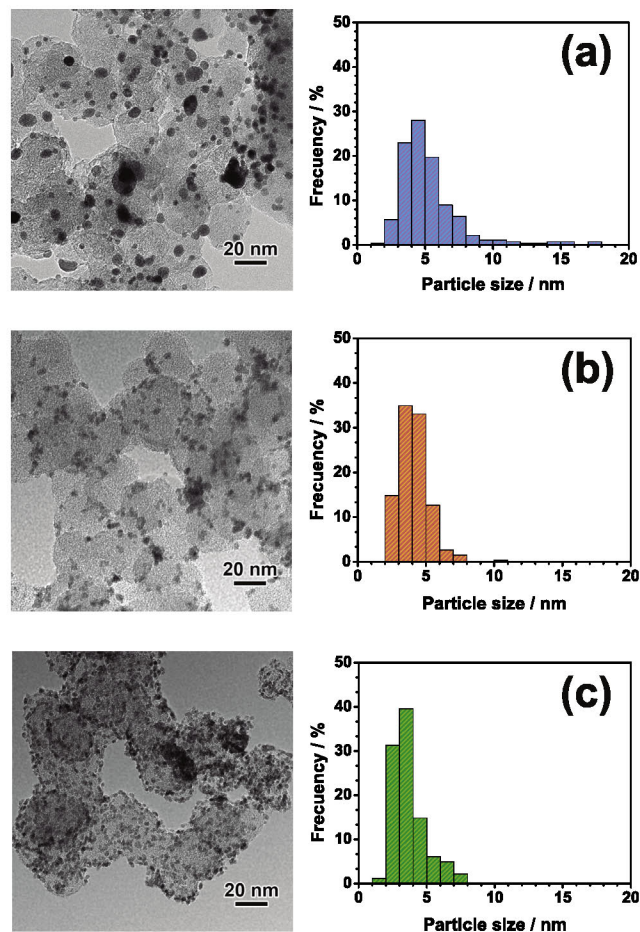


**Fig. 1 – TEM images and histograms of particles size distribution of a PtCo/C, b PtCoRu/C IM and c PtFeRu/C IM.**

region of Co  $2p_{3/2}$ , one at BE = 778 eV ascribed to Co(0) and the other at BE = 781 eV, that could be assigned to CoO (BE = 780 eV), Co(OH)<sub>2</sub> (BE = 780.4 eV) or Co<sub>3</sub>O<sub>4</sub> (BE = 779.6 eV) [29]. A satellite peak at 786 eV can be observed.

The Fe 2p XP spectrum of PtFeRu/C IM catalyst, Fig. 2c, exhibits a complex pattern, which could hardly be deconvoluted into two peaks in the region of Fe  $2p_{3/2}$  at around BE = 707 eV and at around BE = 710.5 eV, composed of photoelectrons from Fe(0), Fe(II) and Fe(III) [30]. Besides, a satellite peak at 712 eV can be observed.

On the other hand, the XP spectra obtained in the region of Ru 3d core-level peak for IM trimetallic catalysts show two components at BE = 280 eV and BE = 281 eV, which can be ascribed to Ru(0) and Ru(IV) [18]. It can be noticed that the Ru 3d core-level peak overlaps with that corresponding to C 1s, which can be deconvoluted into four single peaks associated with different C–C and C–O organic functional groups [31]. Additionally, a satellite peak at ca. 3 eV higher BE than the value for the Ru(IV) main peak can be observed.

### EDS analysis

The EDS atomic percentage ratios of the synthesized catalysts are listed together with XPS atomic percentage ratios in Table

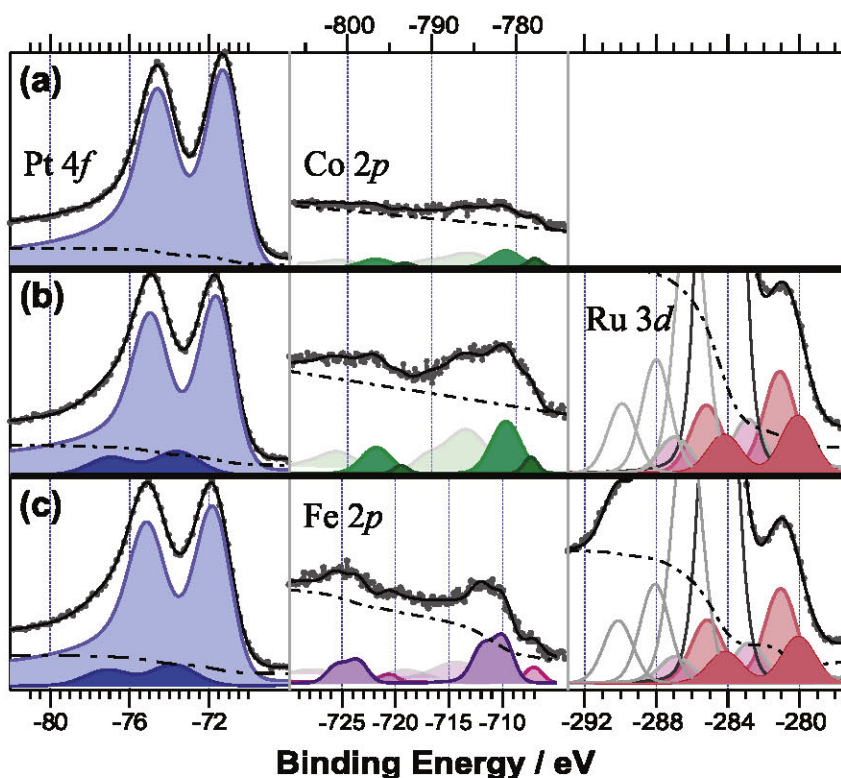


Fig. 2 – XPS spectra of a PtCo/C, b PtCoRu/C IM and c PtFeRu/C.

1. The amounts of Ru and Pt in the IM catalysts are almost the same and those of Co and Fe are about half of them.

XPS and EDS analysis revealed that the amount of the metallic components for PtCoRu/C on the surface and in the bulk is quite similar, although some differences appear for PtFeRu/C, being less the amount of Fe on the surface in reference to the overall composition obtained from EDS.

#### Accelerated stress test

Polarization curves at  $\omega = 2000$  rpm in an  $O_2$ -saturated 0.5 M  $H_2SO_4$  solution for ORR on PtCo/C, PtCoRu/C IM and PtFeRu/C IM electrodes, recorded before and after 2000 potential cycles at  $0.05$   $Vs^{-1}$  between 0.05 V and 0.8 V [32], are shown in Fig. 3a, b and c, respectively. For all tested catalysts, the onset potential values and the specific activities ( $mAcm_{Pt}^{-2}$ ) at 0.8 V for the ORR before and after potential cycling are shown as an inset in each Fig. 3. The polarization curves for ORR with and without methanol after the cycling test are shown in Fig. 4a, b and c. In order to show changes in the

methanol tolerance due to AST, the polarization curves with and without methanol before the treatment are depicted in the inset of each Fig. 4. To study the catalysts stability during AST, cyclic voltammograms were recorded after various numbers of potential cycles and they are shown in Fig. 5 together with the variation of normalized ECSA, i.e. the ECSA determined after the electrochemical experiment, referred to its initial value before AST.

It can be seen that the PtCo/C catalyst suffers strong electrochemically active surface area decay. According to some authors [33–37], the main degradation mechanism related to the deterioration is attributed to sintering and agglomeration of the metallic particles. On the contrary, in the case of the trimetallic PtMRu/C, the ECSA increase with the number of cycles for both PtCoRu/C and PtFeRu/C, which could be attributed to surface roughening and removal of contaminants from the sample surface [25,38].

Both, PtCoRu/C and PtFeRu/C IM exhibit great resistance to changes in their catalytic behavior for ORR after the potential cycling, whereas PtCo/C undergoes a strong decay in its catalytic activity. Even more, the specific activity for ORR after cycling increases up to 30% for trimetallic IM catalysts and decreases about 25% for PtCo/C. In line with this behavior, the onset potentials for ORR shift towards higher potentials for trimetallic IM catalysts and towards lower potentials for PtCo/C after cycling. The decay in performance of PtCo/C catalyst, i.e., specific activity, onset potential, electrochemically active surface area, could be mainly attributed to the particle agglomeration. For the results obtained with PtMRu/C catalysts, a plausible explanation could be an increase in the contribution

Table 1 – EDS and XPS atomic percentage ratios (%) of the synthesized catalysts.

Catalyst	EDS				XPS			
	Pt	Co	Fe	Ru	Pt	Co	Fe	Ru
PtFeRu/C	41		24	35	49		14	37
PtCoRu/C	40	25		35	41	21		38
PtCo/C	91	9			91	9		

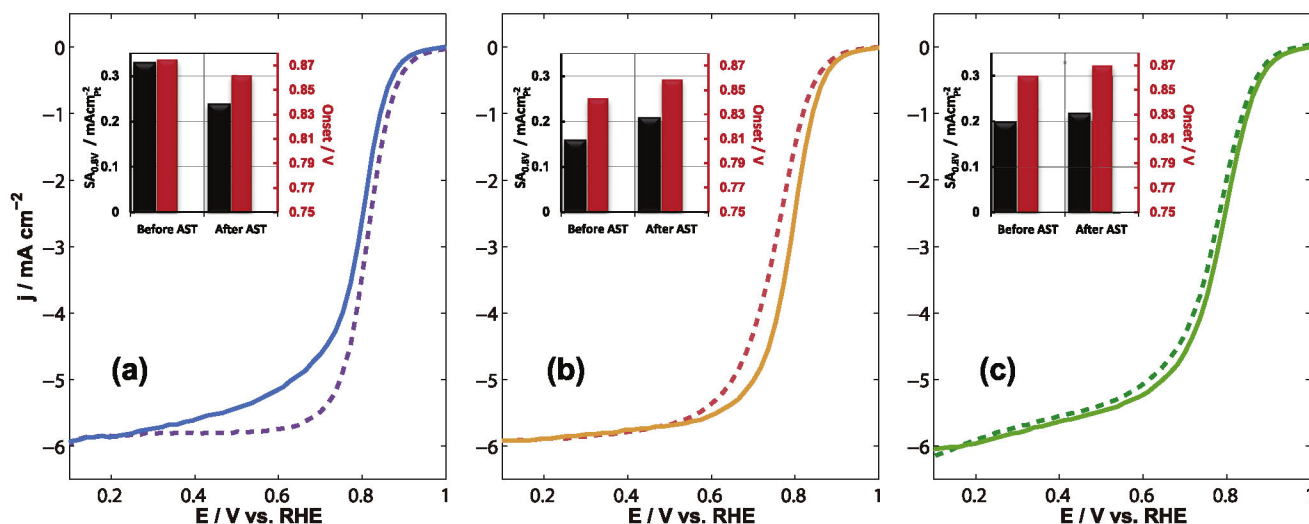


Fig. 3 – Polarization curves for ORR before (---) and after (—) AST on the synthesized catalysts in  $\text{O}_2$  saturated 0.5 M  $\text{H}_2\text{SO}_4$  solution at  $\nu = 0.005 \text{ Vs}^{-1}$  and  $\omega = 2000 \text{ rpm}$  for a PtCo/C, b PtCoRu/C IM and c PtFeRu/C IM. Onset potential for the ORR and specific activity at 0.8 V before and after AST are shown in the respective inset.

of corner and edge sites to total surface sites due to a possible dissolution of less noble components after the AST [39,7].

The persistence of methanol tolerance of the studied catalysts after the AST shown in the inset of Fig. 4, again follows the tendency describes above. Trimetallic IM catalysts have not only a remarkably higher methanol tolerance than PtCo/C before the AST but also keep it after the 2000 electrochemical potential sweeps.

It is important to highlight that after AST the amount of recovered catalyst was very little to analyze in order to detect any morphological changes, with the physical techniques employed in this work. Therefore, the catalyst degradation and methanol tolerance over time were evaluated through their electrochemical behavior.

Despite the fact that the trimetallic PtMRu/C catalysts were subjected to many electrochemical experiences, starting from 1 V, which can be thought as numerous start/stop cycles, the PtMRu/C electrodes have suffered neither drastic catalytic activity deterioration nor methanol tolerance decay. Yet further investigation is needed in order to determine the stability of Ru in these catalysts at higher potentials.

## Conclusions

The IM catalysts have almost the same catalytic behavior as PtCo/C for ORR and, unlike the PtCo/C, are also methanol-tolerant. After the electrochemical accelerated stress test it

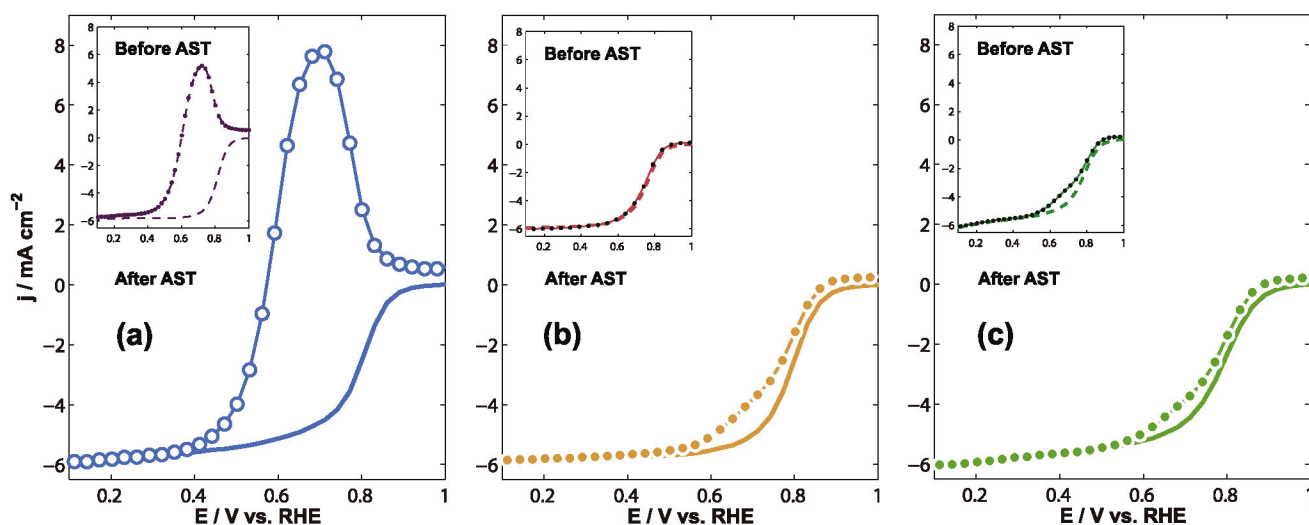
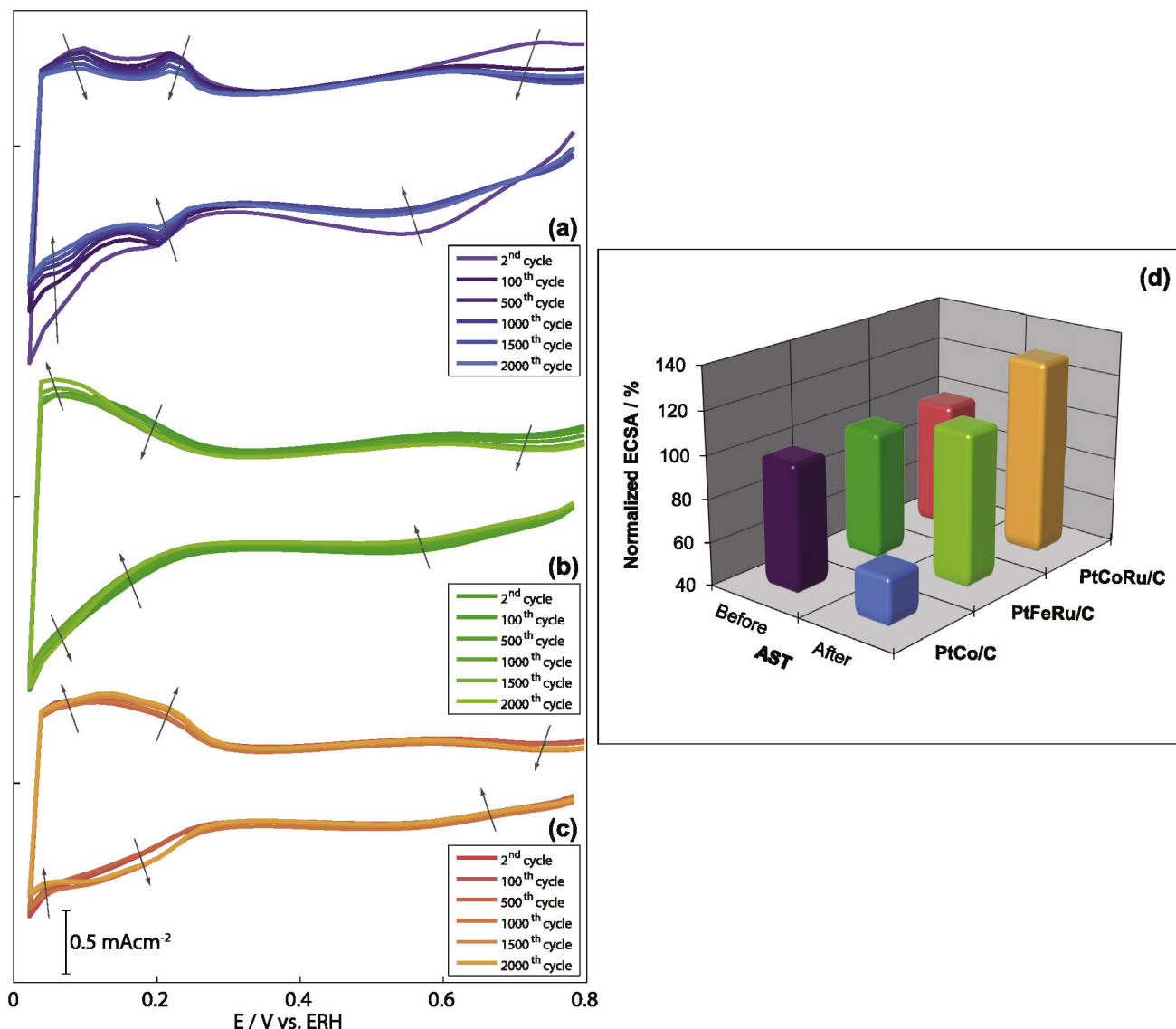


Fig. 4 – Polarization curves for ORR with 0.1 M  $\text{CH}_3\text{OH}$  (---) and without  $\text{CH}_3\text{OH}$  (—) after AST on the synthesized catalysts in  $\text{O}_2$  saturated 0.5 M  $\text{H}_2\text{SO}_4$  solution at  $\nu = 0.005 \text{ Vs}^{-1}$  and  $\omega = 2000 \text{ rpm}$  for a PtCo/C, b PtCoRu/C IM and c PtFeRu/C IM. In the inset the polarization curves before the AST with 0.1 M  $\text{CH}_3\text{OH}$  (---) and without  $\text{CH}_3\text{OH}$  (—) are shown.



**Fig. 5 – Cycling voltammograms recorder in N<sub>2</sub>-purged 0.5 M H<sub>2</sub>SO<sub>4</sub> at 0.05 V<sup>-1</sup> at different numbers of potential cycles a PtCo/C, b PtFeRu/C, c PtCoRu/C and d the variation of normalized ECSA in % before and after AST. Arrows show the changes in the cycling voltammogram profiles over time.**

is found that PtCo/C shows serious decay in its catalytic behavior for ORR and is even less methanol-tolerant, while IM catalysts improve their ORR behavior and adequately maintain their methanol tolerance.

It appears that the studied trimetallic Pt-based catalysts containing Ru, Co or Fe endure the AST and keep their catalytic behavior for ORR in the presence of methanol over time.

## Acknowledgments

This work was supported by Consejo Nacional de Investigaciones Científicas y Técnicas (CONICET), Agencia Nacional de Promoción Científica y Tecnológica, Comisión de Investigaciones Científicas de la Provincia de Buenos Aires (CIC), and Universidad Tecnológica Nacional (UTN-FRLP). AMCL is

member of the research career at CIC. GC and MA acknowledge financial support through a Ph.D. fellowship from CIC and CONICET, respectively.

## REFERENCES

- [1] Corti HR, Gonzalez ER. Direct alcohol fuel cells: materials, performance, durability and applications. Netherlands: Springer; 2014. <http://dx.doi.org/10.1007/978-94-007-7708-8>. URL <http://link.springer.com/book/10.1007/978-94-007-7708-8>.
- [2] Li X, Faghri A. Review and advances of direct methanol fuel cells (DMFCs) part I: design, fabrication, and testing with high concentration methanol solutions. J Power Sources 2013;226:223–40. <http://dx.doi.org/10.1016/j.jpowsour.2012.10.061>. URL <http://linkinghub.elsevier.com/retrieve/pii/S0378775312016175>.

- [3] Baglio V, Stassi A, Matera FV, Antonucci V, Aricò AS. Investigation of passive DMFC mini-stacks at ambient temperature. *Electrochimica Acta* 2009;54(7):2004–9. <http://dx.doi.org/10.1016/j.electacta.2008.07.061>. URL <http://linkinghub.elsevier.com/retrieve/pii/S0013468608009432>.
- [4] Zhang J. PEM fuel cell electrocatalysts and catalyst layers: fundamentals and applications. London: Springer; 2008. <http://dx.doi.org/10.1007/978-1-84800-936-3>.
- [5] Murthi VS, Urian RC, Mukerjee S. Oxygen reduction kinetics in low and medium temperature acid environment: correlation of water activation and surface properties in supported Pt and Pt alloy electrocatalysts. *J Phys Chem B* 2004;108:11011–23. <http://dx.doi.org/10.1021/jp048985k>.
- [6] Escudero-Cid R, Hernández-Fernández P, Pérez-Flores JC, Rojas S, García-Rodríguez S, Fatás E, et al. Analysis of performance losses of direct methanol fuel cell with methanol tolerant PtCoRu/C cathode electrode. *Int J Hydrogen Energy* 2011;36(12):158. URL <http://linkinghub.elsevier.com/retrieve/pii/S0360319911028928>.
- [7] Van Der Vliet DF, Wang C, Li D, Paulikas AP, Greeley J, Rankin RB, et al. Unique electrochemical adsorption properties of Pt-skin surfaces. *Angew Chem - Int Ed* 2012;51:3139–42. <http://dx.doi.org/10.1002/anie.201107668>.
- [8] Gasteiger H a, Kocha SS, Sompalli B, Wagner FT. Activity benchmarks and requirements for Pt, Pt-alloy, and non-Pt oxygen reduction catalysts for PEMFCs. *Appl Catal B Environ* 2005;56(1–2):9–35. <http://dx.doi.org/10.1016/j.apcatb.2004.06.021>. URL <http://linkinghub.elsevier.com/retrieve/pii/S0926337304004941>.
- [9] Ishiguro N, Kityakarn S, Sekizawa O, Uruga T, Sasabe T, Nagasawa K, et al. Rate enhancements in structural transformations of Pt-Co and Pt-Ni bimetallic cathode catalysts in polymer electrolyte fuel cells studied by in situ time-resolved X-ray absorption fine structure. *J Phys Chem C* 2014;118:15874–83. <http://dx.doi.org/10.1021/jp504738p>.
- [10] Sheng W, Lee SW, Crumlin EJ, Chen S, Shao-Horn Y. Synthesis, activity and durability of Pt nanoparticles supported on multi-walled carbon nanotubes for oxygen reduction. 2011. <http://dx.doi.org/10.1149/2.066111jes>.
- [11] Yu P, Pemberton M, Plasse P. PtCo/C cathode catalyst for improved durability in PEMFCs. *J Power Sources* 2005;144:11–20. <http://dx.doi.org/10.1016/j.jpowsour.2004.11.067>.
- [12] Stamenkovic VR, Mun BS, Arenz M, Mayrhofer KJJ, Lucas CA, Wang G, et al. Trends in electrocatalysis on extended and nanoscale Pt-bimetallic alloy surfaces. *Nat Mater* 2007;6:241–7. <http://dx.doi.org/10.1038/nmat1840>.
- [13] Cui C, Gan L, Heggen M, Rudi S, Strasser P. Compositional segregation in shaped Pt alloy nanoparticles and their structural behaviour during electrocatalysis. *Nat Mater* 12 June 2013:765–71. <http://dx.doi.org/10.1038/nmat3668>. URL <http://dx.doi.org/10.1038/nmat3668>, <http://www.ncbi.nlm.nih.gov/pubmed/23770725>.
- [14] Wang D, Zhuang L, Lu J. An alloying-degree-controlling step in the impregnation synthesis of PtRu/C catalysts. *J Phys Chem C* 2007;111:16416–22. <http://dx.doi.org/10.1021/jp073062l>.
- [15] Pal S, Goswami B, Sarkar P. Controlling the shape of nanocrystals. *J Phys Chem C* 2007;111:16071–5. <http://dx.doi.org/10.1021/jp074950j>.
- [16] Han B, Carlton CE, Kongkanand A, Kukreja RS, Theobald BR, Gan L, et al. Record activity and stability of dealloyed bimetallic catalysts for proton exchange membrane fuel cells. *Energy Environ Sci* 2015;8:258–66. <http://dx.doi.org/10.1039/C4EE02144D>. URL <http://xlink.rsc.org/?DOI=C4EE02144D>.
- [17] Wang C, Chi M, Li D, Van Der Vliet D, Wang G, Lin Q, et al. Synthesis of homogeneous Pt-bimetallic nanoparticles as highly efficient electrocatalysts. *ACS Catal* 2011;1:1355–9. <http://dx.doi.org/10.1021/cs200328z>.
- [18] Asteazarán M, Bengió S, Triaca WE, Castro Luna AM. Methanol tolerant electrocatalysts for the oxygen reduction reaction. *J Appl Electrochem* 2014;44:1271–8. <http://dx.doi.org/10.1007/s10800-014-0748-1>. URL <http://link.springer.com/10.1007/s10800-014-0748-1>.
- [19] M. Asteazarán, G. Cespedes, S. Bengió, M. Moreno, W. Triaca, A. M. Castro Luna, Research on methanol-tolerant catalysts for the oxygen reduction reaction, *Journal of Applied Electrochemistry* (in press). doi:<http://dx.doi.org/10.1007/s10800-015-0845-9>.
- [20] Mayrhofer KJJ, Ashton SJ, Meier JC, Wiberg GKH, Hanzlik M, Arenz M. Non-destructive transmission electron microscopy study of catalyst degradation under electrochemical treatment. *J Power Sources* 2008;185:734–9. <http://dx.doi.org/10.1016/j.jpowsour.2008.08.003>.
- [21] Zhang Y, Chen S, Wang Y, Ding W, Wu R, Li L, et al. Study of the degradation mechanisms of carbon-supported platinum fuel cells catalyst via different accelerated stress test. *J Power Sources* 2015;273:62–9. <http://dx.doi.org/10.1016/j.jpowsour.2014.09.012>. URL <http://linkinghub.elsevier.com/retrieve/pii/S0378775314014189>.
- [22] Zhang S, Yuan X, Wang H, Mérida W, Zhu H, Shen J, et al. A review of accelerated stress tests of MEA durability in PEM fuel cells. 2009. <http://dx.doi.org/10.1016/j.ijhydene.2008.10.012>.
- [23] Spanos I, Kirkensgaard JJK, Mortensen K, Arenz M. Investigating the activity enhancement on Pt<sub>x</sub>Co<sub>1-x</sub> alloys induced by a combined strain and ligand effect. *J Power Sources* 2014;245:908–14. <http://dx.doi.org/10.1016/j.jpowsour.2013.07.023>. URL <http://linkinghub.elsevier.com/retrieve/pii/S0378775313012032>.
- [24] Salgado J, Antolini E, Gonzalez E. Structure and activity of carbon-supported PtCo electrocatalysts for oxygen reduction. *J Phys Chem B* 2004;108(46):17767–74. <http://dx.doi.org/10.1021/jp0486649>. URL <http://pubs.acs.org/doi/abs/10.1021/jp0486649>.
- [25] Wang D, Xin HL, Yu Y, Wang H, Rus E, Muller D a, et al. Pt-decorated PdCo@Pd/C core-shell nanoparticles with enhanced stability and electrocatalytic activity for the oxygen reduction reaction. *J Am Chem Soc* 2010;132(50):17664–6. <http://dx.doi.org/10.1021/ja107874u>. URL <http://www.ncbi.nlm.nih.gov/pubmed/21105661>.
- [26] Vielstich W, Lamm A, Gasteiger HA. *Handbook of fuel cells - fundamentals, technology, and applications*. Hoboken: John Wiley & Sons; 2003.
- [27] Garsany Y, Baturina OA, Swider-Lyons KE, Kocha SS. Experimental methods for quantifying the activity of platinum electrocatalysts for the oxygen reduction reaction. *Anal Chem* 2010;82(15):6321–8. <http://dx.doi.org/10.1021/AC100306C>. URL <http://www.ncbi.nlm.nih.gov/pubmed/20590161>.
- [28] Aricò AS, Shukla AK, Kim H, Park S, Min M, Antonucci V. XPS study on oxidation states of Pt and its alloys with Co and Cr and its relevance to electroreduction of oxygen. *Appl Surf Sci* 2001;172(1–2):33–40. [http://dx.doi.org/10.1016/S0169-4332\(00\)00831-X](http://dx.doi.org/10.1016/S0169-4332(00)00831-X). URL <http://www.sciencedirect.com/science/article/pii/S016943320000831X>, <http://linkinghub.elsevier.com/retrieve/pii/S0022072801004211>, <http://linkinghub.elsevier.com/retrieve/pii/S016943320000831X>.
- [29] Biesinger MC, Payne BP, Grosvenor AP, Lau LWM, Gerson AR, Smart RSC. Resolving surface chemical states in XPS analysis of first row transition metals, oxides and hydroxides: Cr, Mn, Fe, Co and Ni. *Appl Surf Sci* 2011;257:2717–30. <http://dx.doi.org/10.1016/j.apsusc.2010.10.051>.

- [30] Grosvenor AP, Kobe BA, Biesinger MC, McIntyre NS. Investigation of multiplet splitting of Fe 2p XPS spectra and bonding in iron compounds. *Surf Interface Analysis* 2004;36:1564–74. <http://dx.doi.org/10.1002/sia.1984>.
- [31] Vivo-Vilches JF, Bailón-García E, Pérez-Cadenas AF, Carrasco-Marín F, Maldonado-Hódar FJ. Tailoring the surface chemistry and porosity of activated carbons: evidence of reorganization and mobility of oxygenated surface groups. *Carbon* 2014;68:520–30. <http://dx.doi.org/10.1016/j.carbon.2013.11.030>.
- [32] Matsuoka K, Sakamoto S, Fukunaga A. Degradation of membrane electrode assemblies utilizing PtRu catalysts under high potential conditions. *J Power Sources* 2013;238:251–6. <http://dx.doi.org/10.1016/j.jpowsour.2013.03.058>.
- [33] Büchi FN, Inaba M, Schmidt TJ. *Polymer electrolyte fuel cell durability*. New York, NY: Springer; 2009. <http://dx.doi.org/10.1007/978-0-387-85536-3>. URL <http://link.springer.com/10.1007/978-0-387-85536-3>.
- [34] Antolini E, Salgado JR, Gonzalez ER. The stability of PtM (M=first row transition metal) alloy catalysts and its effect on the activity in low temperature fuel cells. *J Power Sources* 2006;160(2):957–68. <http://dx.doi.org/10.1016/j.jpowsour.2006.03.006>. URL <http://linkinghub.elsevier.com/retrieve/pii/S0378775306004216>.
- [35] Zhang S, Yuan X-Z, Hin JNC, Wang H, Friedrich KA, Schulze M. A review of platinum-based catalyst layer degradation in proton exchange membrane fuel cells. *J Power Sources* 2009;194(2):588–600. <http://dx.doi.org/10.1016/j.jpowsour.2009.06.073>. URL <http://linkinghub.elsevier.com/retrieve/pii/S037877530901146X>.
- [36] Ferreira PJ, la O GJ, Shao-Horn Y, Morgan D, Makharia R, Kocha S, et al. Instability of Pt/C electrocatalysts in proton exchange membrane fuel cells - a mechanistic investigation. *J Electrochem Soc* 2005;152:A2256–71. <http://dx.doi.org/10.1149/1.2050347>. URL <Go to ISI>://000233133700023.
- [37] Wu J, Yuan XZ, Martin JJ, Wang H, Zhang J, Shen J, et al. A review of PEM fuel cell durability: degradation mechanisms and mitigation strategies. 2008. <http://dx.doi.org/10.1016/j.jpowsour.2008.06.006>.
- [38] Hodnik N, Zorko M, Bele M, Hočevar S, Gabersček M. Identical location scanning electron microscopy: a case study of electrochemical degradation of PtNi nanoparticles using a new nondestructive method. *J Phys Chem C* 2012;116(40):21326–33. <http://dx.doi.org/10.1021/jp303831c>. URL <http://pubs.acs.org/doi/abs/10.1021/jp303831c>.
- [39] Li X, Chen Q, McCue I, Snyder J, Crozier P, Erlebacher J, et al. Dealloying of noble-metal alloy nanoparticles. *Nano Lett* 2014;14:2569–77. <http://dx.doi.org/10.1021/nl500377g>.